JURNAL MIPA 13 (2) 71-77

dapat diakses melalui
https://ejournal.unsrat.ac.id/v3/index.php/jmuo/index

Determining the Coefficient of Restitution for Imperfect Elastic Collisions between Glass Marbles and Ceramic Surfaces using Time-Lapse Videography

Mahendra Kusuma Nugraha[a]*, Ernawatil Gani[a], Jumriadi[a]

[a]Physics Department, Faculty of Mathematics and Natural Sciences, Sam Ratulangi University, Indonesia

KATA KUNCI

Kelereng
Tumbukan elastis
Koefisien restitusi
Videografi jeda-waktu

ABSTRAK

Untuk menyelami potensi lanjut dari videografi jeda-waktu, metode ini digunakan untuk mengamati dinamika tumbukan jatuh bebas elastis tak sempurna antara kelereng kaca dan lantai keramik, menggunakan kamera ponsel SHARP® Aquos Sense 4+ dengan kecepatan rana 30 kerangka per detik. Peristiwa-peristiwa tersebut direkam dan dianalisis menggunakan metode pemisahan kerangka, yang kemudian diamati secara visual untuk menentukan tinggi setiap pantulan. Analisis mengungkapkan bahwa koefisien restitusi rata-rata untuk tabrakan tersebut adalah $\bar{\varepsilon}_{1st} \cong 0.86$ dan $\bar{\varepsilon}_{2nd} \cong 0.843$, dengan tinggi jatuh bebas awal masing-masing adalah 20.3 cm dan 16.2 cm untuk percobaan pertama dan kedua. Eksperimen-eksperimen ini menggambarkan bahwa setiap peristiwa menunjukkan sebuah tumbukan elastis yang tidak sempurna, menunjukkan bagaimana energi mekanik tersebar dari kelerang ke sekitarnya karena ε tidak sama dengan 1. Variasi kecil dalam hasil koefisien terjadi karena batasan yang diberlakukan oleh hukum termodinamika.

KEYWORDS

Marble
Elastic collision
Restitution coefficient
Time-lapse videography

ABSTRACT

To explore and delve into the potential of time-lapse videography, this method was employed to observe the dynamics of imperfect elastic free-fall collisions between a standard glass marble and a ceramic-tiled floor surface, using a SHARP® Aquos Sense 4+ smartphone camera with a shutter speed of 30 frames per second (fps). The events were recorded and analysed using the frame-splitting method, which was then visually observed to determine the height of each bounce. The analysis revealed that the average coefficients of restitution for the collisions were $\bar{\varepsilon}_{1st} \cong 0.86$ *and* $\bar{\varepsilon}_{2nd} \cong 0.843$*, with the initial free-fall heights being 20.3 cm and 16.2 cm respectively for the first and second trials. These experiments illustrate that every event signifies an imperfect elastic collision, showing how mechanical energy dissipates from the marble into its surroundings since ε is not equal to 1. The slight variations in the coefficient outcomes occur due to the constraints imposed by the laws of thermodynamics.*

TERSEDIA *ONLINE*

01 Agustus 2024

Introduction

Time-lapse imaging, also known as time lapse photography, is a technique in which a series of photographs are captured at specific intervals over a period of time and then played back at a faster rate than they were taken. This sequence of time-lapse images can be used to extract information and characteristics contained within them, which can then be comprehensively analysed to understand physical events or phenomena under investigation or observation, whether directly or with the assistance of additional equipment. It also creates a video or sequence of images that compress time, allowing

*Corresponding author:
Email address: mahendrakusuma@unsrat.ac.id
Published by FMIPA UNSRAT (2024)

viewers to observe changes that occur slowly over time, such as the growth of plants, the movement of clouds, construction progress, or other dynamic processes (Persohn 2015; Vollmer and Möllmann 2018a, 2018b; Yang et al. 2015).

In time-lapse imaging or time-lapse videography, the interval between each photograph, known as the frame interval, can vary depending on the desired effect and the speed at which the final video or sequence should be played back. Time-lapse imaging is widely used in various fields, including filmmaking, scientific research, construction monitoring, and creative art projects, to document and visualize gradual changes or processes that might not be easily observable in real time. In essence, time-lapse imaging shares similarities with time-lapse photography in terms of acquiring a series of images or frames (Abeid and Arditi 2002; Liu and Li 2012; Mursalim, Atmajaya, and Alwi 2021; Vera et al. 2016). However, the key difference lies in the use of very short exposure times and a high frame rate per second to capture all the details of the observed phenomenon in the resulting images. The higher the frame rate per second, the sharper the time-lapse images produced. Additionally, time-lapse imaging can be combined with various image reconstruction techniques such as Fourier transform and filtered back-projection to facilitate analysis and enhance the acquisition of information and characteristics related to the observed physical phenomenon (Baroutsis 2020; Kramer and Wohl 2014; Revuelto, Jonas, and López-Moreno 2016).

The technology and methods of time-lapse imaging have found widespread use in various research and experimental fields, including physics (Liu and Li 2012; Rubinstein et al. 2011), medicine (Chen et al. 2013; Urbano et al. 2017), geography (Huintjes et al. 2015; Kenner et al. 2018), and education (Liu and Li 2012; Persohn 2015; Vollmer and Möllmann 2018b). This experiment was conducted to directly observe the manifestations of imperfect elastic collision interactions that occur during collisions between glass marbles of different sizes and masses against a flat surface. One of the main outcomes sought from this experiment is the coefficient of restitution for the glass marbles in question. Another parameter worth observing and analyzing is the type of flat surface used as the medium for these imperfect elastic collision interactions.

The essence of this entire experiment was to investigate and explore the potential of a basic and straightforward time-lapse videography setup as a method and modality for directly visualizing various physical phenomena. It is anticipated that this could prove valuable for researchers and even students in schools.

Methods and Material

The research methodology consists of three stages: equipment and material preparation, experimental setup arrangement, data analysis methods, and discussion. The experiments will take place in the Integrated Laboratory of the Physics Unit at Sam Ratulangi University. During the preparation phase, various components required for the experiment will be assembled, including the glass marbles, millimetre ruler, stand and supports, a SHARP® Aquas Sense 4+ smartphone, and an Asus® BR1100FKA 4/128 2C 1.1 GHz portable laptop used as hardware for data processing and analysis. The marbles have an average density of 2.5 g/cm³ to 2.6 g/cm³, and the diameter was around ± 13 mm. Additionally, computer software applications, such as Wonders hare Filmora9® and Video to JPG Converter®, will be utilized for data analysis, and they are freely available for Windows®. The experimental setup scheme is illustrated in **Figure 1.** below.

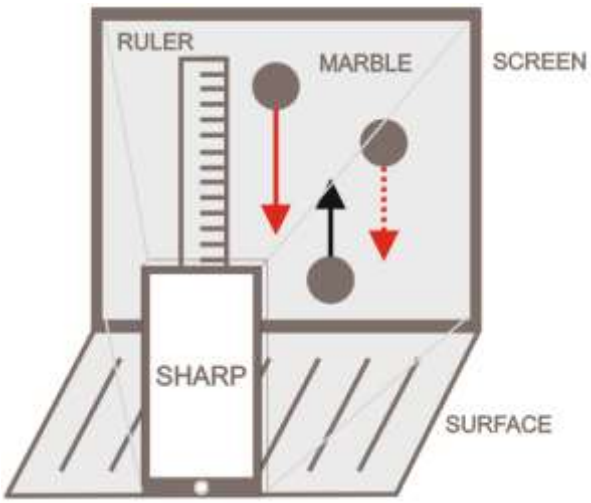

Figure 1. Schematic design of a onefold time-lapse imaging modality.

The data analysis phase begins with the formulation of an experimental procedure. This procedure involves several steps, including configuring the camera's image settings, determining the initial height from which the marble will be dropped, ensuring the camera's position aligns with the marble's collision path, installing software applications on the laptop, recording the phenomenon, processing the image data, and observing and measuring the maximum bounce height for each reflection based on the captured images.

A foundational understanding of several key principles is essential before experimenting. These principles include the laws governing the conservation of mechanical energy, the dynamics of elastic and inelastic collisions, and the coefficient of restitution (ε).

The coefficient of restitution (ε) serves as a quantifiable measure resulting from the application of the conservation of mechanical energy when a rigid object collides with a solid surface and experiences a rebound. Notably, the coefficient of restitution lacks dimensional units and exists solely for quantitatively comparing the mechanical energy before and after the collision.

The collision and rebound phenomena induce changes in gravitational potential energy due to variations in the object's position, both before and after the rebound. Beyond its impact on gravitational potential energy, these positional differences also influence the object's kinetic energy during the entire event. Consequently, the relationship between gravitational potential energy and the object's kinetic energy is inherently connected to the principle of the conservation of mechanical energy.

The coefficient of restitution (ε) typically falls between 0 and 1, with positive values. It relates to specific parameters. When $\varepsilon = 0$, it represents a scenario of perfectly inelastic collisions, where all kinetic energy is converted into heat or work, fully dissipating into the surrounding environment. For values between 0 and 1 ($0 < \varepsilon < 1$), we have partially inelastic collisions, where some kinetic energy is dissipated to the environment. When $\varepsilon = 1$, it indicates perfectly elastic collisions, where no kinetic energy is dissipated, resulting in both objects bouncing back with identical relative velocities. Achieving this ideal scenario in the real world is unattainable due to the constraints imposed by the laws of thermodynamics, which regulate entropy.

In a general sense, the mathematical expression that represents the coefficient of restitution (ε) in the context of this experiment can be outlined as in Equation (1) shown below:

$$\varepsilon = \sqrt{\frac{KE_v}{KE_u}} \tag{1}$$

Equation (1) becomes Equation (2) by plotting the kinetic energy of the object before and after the collision, as given below:

$$\varepsilon = \sqrt{\frac{\left(\frac{1}{2}\right)mv^2}{\left(\frac{1}{2}\right)mu^2}} \tag{2}$$

The mass (m) in Equation (2) is eliminated, resulting in Equation (3) as follows:

$$\varepsilon = \sqrt{\frac{v^2}{u^2}} \tag{3}$$

Equation (3) describes how the coefficient of restitution is determined by comparing the free fall velocities at each position before (u) and after (v) a collision takes place. Let's consider an ideal object undergoing free fall without any air resistance, experiencing an acceleration of g due to gravitational potential energy of $PE = mgH$, where m represents the object's mass. Consequently, the final velocities before (u) and after (v) the collision at each maximum height (H_u and H_v) are expressed in Equation (4) and Equation (5) shown below:

$$v^2 = v_o^2 + 2gH_v \tag{4}$$

$$u^2 = u_o^2 + 2gH_u \tag{5}$$

By plotting (4) and (5) into (3), the formula can be written as Equation (6):

$$\varepsilon = \sqrt{\frac{v^2}{u^2}} = \sqrt{\frac{v_o^2 + 2gH_v}{u_o^2 + 2gH_u}} \tag{6}$$

It is known that the initial velocity of the free-falling object is zero, so Equation (6) can be written as in Equation (7) given below:

$$\varepsilon = \sqrt{\frac{2gH_v}{2gH_u}} \tag{7}$$

The standard acceleration of gravity cancels out, giving birth to Equation (8):

$$\varepsilon = \sqrt{\frac{H_v}{H_u}} \tag{8}$$

Equation (8) will be employed to ascertain the coefficient of restitution after collecting data on the object's rebound height through the process of capturing time intervals. The resulting coefficient of restitution can then serve as an indicator of the specific type of collision event, whether it is perfectly elastic, inelastic, or non-elastic in nature.

Results and Discussions

First Trial

This section provides an examination of the measurement data, which includes the initial height, the first bounce height, and the second bounce height. These height measurements are utilized to compute the coefficient of restitution (ε) for the glass marble in this experiment. **Figure 2.** below shows the time interval imagery of the glass marble's motion as it falls from its initial height and bounces for the first and second time. Based on visual observation of the marble's height under different conditions from every extracted frame, the precise initial height of the marble in the first trial is determined to be $H_u = 20.3 \pm 0.05$ cm. At the same time, the marble's precise maximum height after the first and second bounce is $H_{v_1} = 14.9 \pm 0.05$ cm and $H_{v_2} = 11.1 \pm 0.05$ cm.

Calculation of the restitution coefficient (ε) can then be done by entering the height measurement data into Equation (8) as presented below:

$$\varepsilon_{uv_1} = \sqrt{\frac{H_{v_1}}{H_u}} = \sqrt{\frac{14.9}{20.3}} \tag{9}$$

$$\varepsilon_{uv_1} = \sqrt{0.734} \cong 0.857 \quad (10)$$

$$\varepsilon_{v_{1v_2}} = \sqrt{\frac{H_{v_2}}{H_{v1}}} = \sqrt{\frac{11.1}{14.9}} \quad (11)$$

$$\varepsilon_{v_{1v_2}} = \sqrt{0.745} \cong 0.863 \quad (12)$$

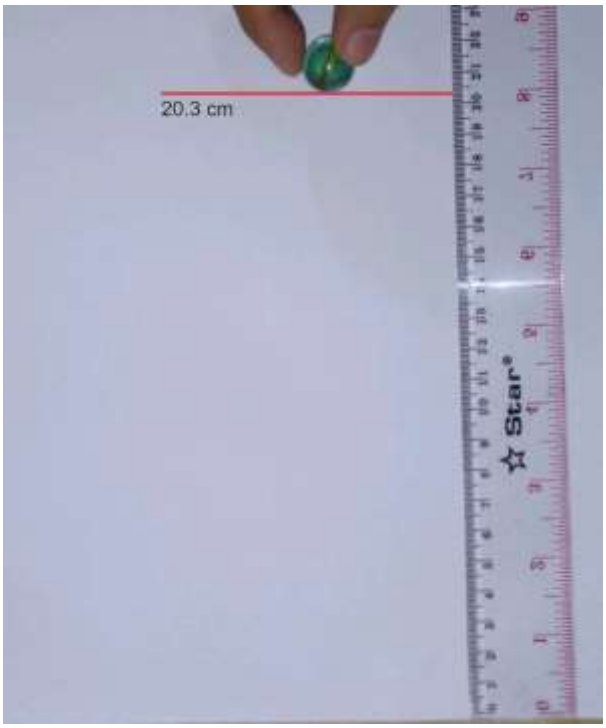

(a)

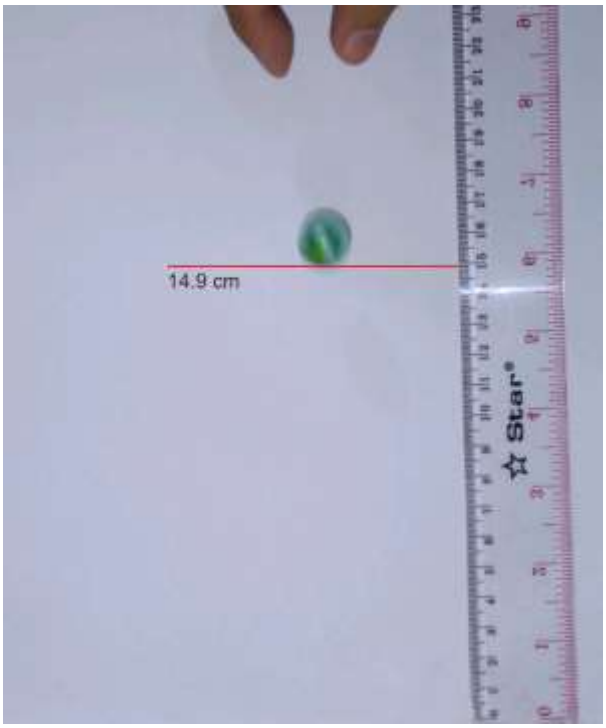

(b)

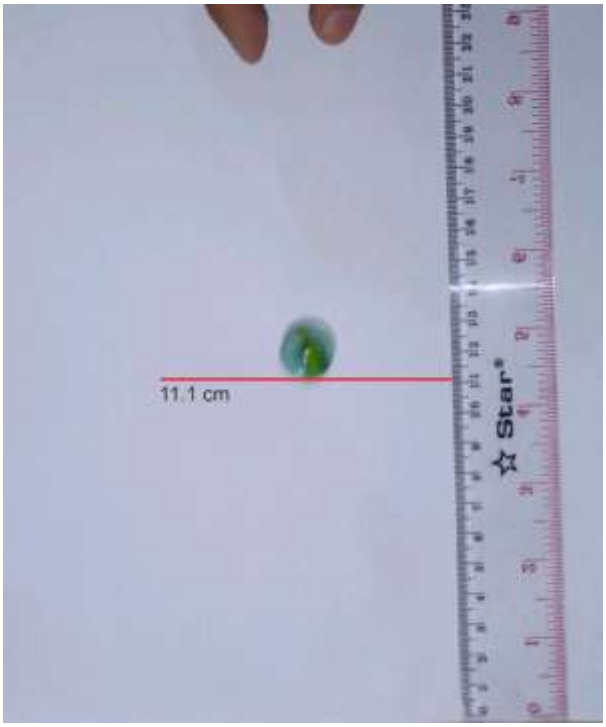

(c)

Figure 2. Image of the marble at the initial height (H_u) (a), image of the marble at maximum height; (b) of the first bounce (H_{v1}) and (c) of the second bounce (H_{v2}). First trial.

The coefficient of restitution, respectively, calculated from the initial height of H_u to the first bounce height of H_{v_1} and from the first bounce height of H_{v1} to the second bounce height of H_{v2} is approximately $e_{uv_1} \cong 0.857$ and $e_{v_{1v_2}} \cong 0.863$. Therefore, the mean coefficient of restitution ($\bar{\varepsilon}_{1st}$) calculated from multiple collisions between the marble and the floor, taking into account the highest points reached during each bounce as in this first trial, is as follows:

$$\bar{\varepsilon}_{1st} = \frac{1}{2}\left(\varepsilon_{uv_1} + \varepsilon_{v_2v_1}\right) \approx 0.86 \quad (13)$$

The difference (deviation) between the two obtained coefficient of restitution values $e_{uv_1} \cong 0.857$ and $e_{v_{1v_2}} \cong 0.863$ is approximately 0.006. This value is considered to be minor concerning the final calculation results, signifying that the measurements conducted were sufficiently accurate and precise. The variance in the restitution coefficient values derived from each collision event is also attributed to the dissipation of mechanical energy exhibited by the marble upon impact with the floor.

It is believed that environmental factors, such as micro-vibrations on the ground surface resulting from human activity or natural occurrences, exert a negligible disturbance on the impact phenomenon. These disturbances contribute to variations in coefficient values. Similarly, it is thought that wind speed can also have a comparable disruptive effect.

Second Trial

Additionally, **Figure 3.**, shown below, displays images capturing the marble's motion during free fall at the initial height (H_u), at the first bounce (H_{v_1}) and at the second bounce (H_{v_2}) in the second trial. From the figure, the precise initial height of the marble in can be seen to be $H_u = 16.2 \pm 0.05$ cm. Meanwhile, the precise maximum height after the bounces, respectively, is about $H_{v_1} = 11.8 \pm 0.05$ cm and $H_{v_2} = 8.2 \pm 0.05$ cm.

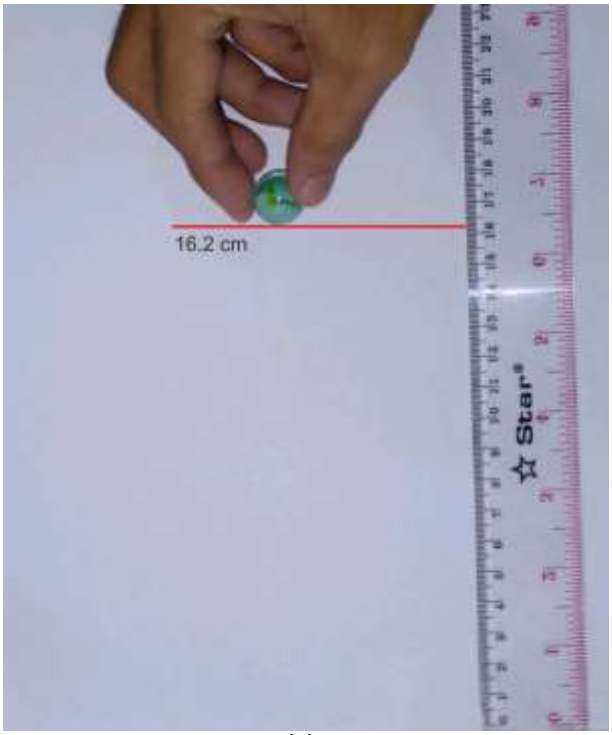

(a)

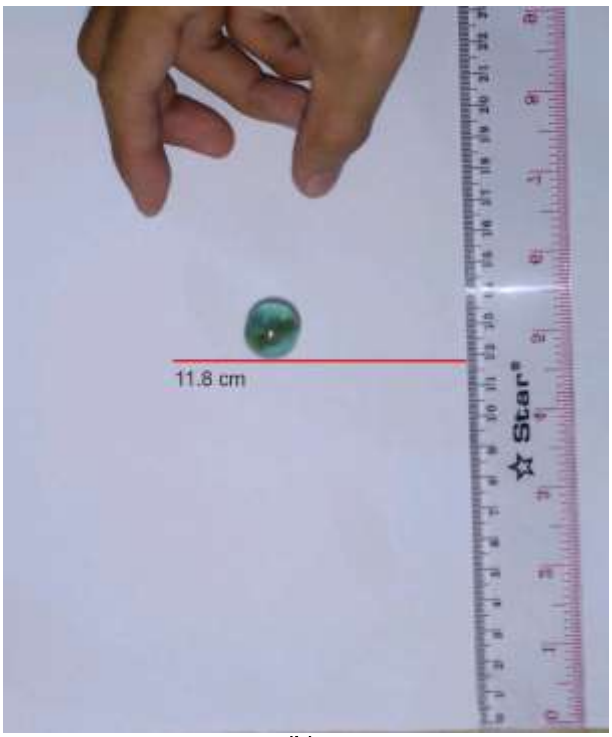

(b)

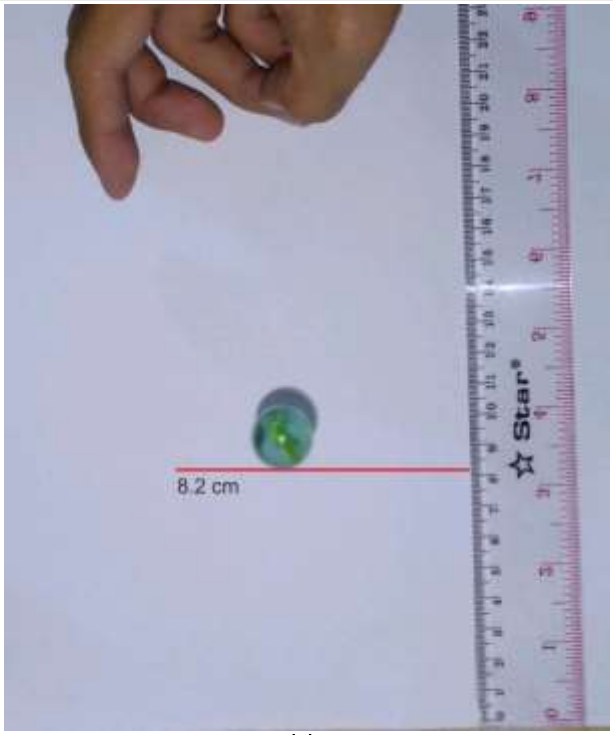

(c)

Figure 3. Image of the marble at the initial height (H_u) (a), image of the marble at maximum height; (b) of the first bounce (H_{v1}) and (c) of the second bounce (H_{v2}). Second trial.

Consistent with previous calculations, the coefficient of restitution can be determined as well by plugging data into the equation, as provided below:

$$\varepsilon_{uv_1} = \sqrt{\frac{H_{v_1}}{H_u}} = \sqrt{\frac{11.8}{16.2}} \tag{14}$$

$$\varepsilon_{uv_1} = \sqrt{0.728} \cong 0.853 \tag{15}$$

$$\varepsilon_{v_1v_2} = \sqrt{\frac{H_{v_2}}{H_{v1}}} = \sqrt{\frac{8.2}{11.8}} \tag{16}$$

$$\varepsilon_{v_1v_2} = \sqrt{0.695} \cong 0.833 \tag{17}$$

In this trial, the restitution coefficient (ε) value obtained from the calculations that has been carried out, respectively, from the initial height of H_u to the first bounce height of H_{v_1} and from the first bounce height of H_{v1} to the second bounce height of H_{v2} is $e_{uv_1} \cong 0.853$ and $e_{v_1v_2} \cong 0.833$. The mean value of the coefficients ($\bar{\varepsilon}_{2nd}$) obtained in this trial is about $\bar{\varepsilon}_{2nd} \cong 0.843$, as is given below:

$$\bar{\varepsilon}_{2nd} = \frac{1}{2}\left(\varepsilon_{uv_1} + \varepsilon_{v_2v_1}\right) \approx 0.843 \tag{18}$$

The deviation between the two values, which are $e_{uv_1} \cong 0.853$ and $e_{v_{1v_2}} \cong 0.833$ is approximately 0.02. This value is almost one order higher than the value obtained from the first trial. Nevertheless, it seems that the coefficient values obtained from one set of events to another have adhered to the principles and physical traits of imperfect elastic collisions.

The variations in decimal values of coefficient results are attributed to momentum transfer fluctuations between collisions, representing real-world manifestations of entropy and thermodynamic laws. Despite these variations, they are not significant enough to invalidate the overall accuracy of the observations and calculations made.

Visual Representation

Additional detailed information regarding the position and height of the marble on the ceramic floor during each impact, in both the initial and subsequent trials, is depicted in **Figure 4.** below:

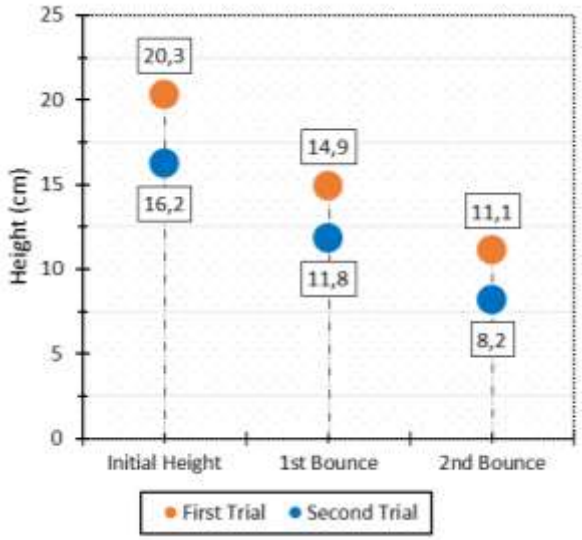

Figure 4. The marble's height at each collision, in both the initial and subsequent trials.

It is evident that the height of each successive bounce is lower than the previous one, as well as the initial height. This represents a tangible manifestation of thermodynamic influence, where energy dissipation transforms a portion of the marble's total mechanical energy into heat energy, which disperses across the surface of the ceramic floor.

Conclusion

Time-lapse videography was employed to observe the interactions during free-fall collisions between a glass marble and a tiled floor surface, using a simple setup. In the initial trial, the average coefficient of restitution for the glass marble was approximately $\varepsilon_{1st} \cong 0.86$, with the marble dropped from a height $of\ H_u = 20.3 \pm 0.05$ cm. The second trial yielded a slightly different coefficient value of approximately $\varepsilon_{2nd} \cong 0.843$, with the marble's initial free-fall height determined to be $H_u = 16.2 \pm 0.05$ cm. These trials demonstrate that each occurrence represents an imperfect elastic collision phenomenon, indicating the dissipation of mechanical energy from the marble into its surroundings as ε is not equal to 1. The negligible differences in the coefficient results exist because of the confines of the laws of thermodynamics.

This experiment presents an opportunity to employ the observation method of objects in free fall motion and calculating the coefficient of restitution through time-lapse videography. It aims to explore the characteristics and, importantly, the quality of ceramics tiles or similar flooring materials. This technique is considered an alternative method that is quick, proper, and cost-effective.

Bibliography

Abeid, Jorge, and David Arditi. 2002. "Time-Lapse Digital Photography Applied to Project Management." *Journal of Construction Engineering and Management* 128(6):530–35. doi: 10.1061/(asce)0733-9364(2002)128:6(530).

Baroutsis, Aspa. 2020. "Sociomaterial Assemblages, Entanglements and Text Production: Mapping Pedagogic Practices Using Time-Lapse Photography." *Journal of Early Childhood Literacy* 20(4):732–54. doi: 10.1177/1468798418784128.

Chen, Alice A., Lei Tan, Vaishali Suraj, Renee Reijo Pera, and Shehua Shen. 2013. "Biomarkers Identified with Time-Lapse Imaging: Discovery, Validation, and Practical Application." *Fertility and Sterility* 99(4):1035–43. doi: 10.1016/j.fertnstert.2013.01.143.

Huintjes, Eva, Tobias Sauter, Benjamin Schroter, Fabien Maussion, Wei Yang, Jan Kropaček, Manfred Buchroithner, Dieter Scherer, Shichang Kang, and Christoph Schneider. 2015. "Evaluation of a Coupled Snow and Energy Balance Model for Zhadang Glacier, Tibetan Plateau, Using Glaciological Measurements and Time-Lapse Photography." *Arctic, Antarctic, and Alpine Research* 47(3):573–90. doi: 10.1657/AAAR0014-073.

Kenner, Robert, Marcia Phillips, Philippe Limpach, Jan Beutel, and Martin Hiller. 2018. "Monitoring Mass Movements Using Georeferenced Time-Lapse Photography: Ritigraben Rock Glacier, Western Swiss Alps." *Cold Regions Science and Technology* 145(1):127–34. doi: 10.1016/j.coldregions.2017.10.018.

Kramer, Natalie, and Ellen Wohl. 2014. "Estimating Fluvial Wood Discharge Using Time-Lapse Photography with Varying Sampling Intervals." *Earth Surface Processes and Landforms* 39(6):844–52. doi: 10.1002/esp.3540.

Liu, Wei, and Hongyun Li. 2012. "Time-Lapse Photography Applied to Educational Videos." *2012 2nd International Conference on Consumer Electronics, Communications and Networks, CECNet 2012 - Proceedings* 2(1):3669–72. doi: 10.1109/CECNet.2012.6202303.

Mursalim, Muh. Ainun Amri, Dedy Atmajaya, and Erick Irawadi Alwi. 2021. "Pengembangan Alat Bantu Timelapse Photography Berbasis Arduino." *Buletin Sistem Informasi Dan Teknologi Islam* 2(1):17–20. doi: 10.33096/busiti.v2i1.718.

Persohn, Lindsay. 2015. "Exploring Time-Lapse Photography as a Means for Qualitative Data Collection." *International Journal of Qualitative Studies in Education* 28(5):501–13. doi: 10.1080/09518398.2014.915999.

Revuelto, Jesús, Tobias Jonas, and Juan Ignacio López-Moreno. 2016. "Backward Snow Depth Reconstruction at High Spatial Resolution Based on Time-Lapse Photography." *Hydrological Processes* 30(17):2976–90. doi: 10.1002/hyp.10823.

Rubinstein, Michael, Ce Liu, Peter Sand, Frědo Durand, and William T. Freeman. 2011. "Motion Denoising with Application to Time-Lapse Photography." *Proceedings of the IEEE Computer Society Conference on Computer Vision and Pattern Recognition* 1(1):313–20. doi: 10.1109/CVPR.2011.5995374.

Urbano, Leonardo F., Puneet Masson, Matthew Vermilyea, and Moshe Kam. 2017. "Automatic Tracking and Motility Analysis of Human Sperm in Time-Lapse Images." *IEEE Transactions on Medical Imaging* 36(3):792–801. doi: 10.1109/TMI.2016.2630720.

Vera, Rodrigo Hernández, Emil Schwan, Nikos Fatsis-Kavalopoulos, and Johan Kreuger. 2016. "A Modular and Affordable Time-Lapse Imaging and Incubation System Based on 3D-Printed Parts, a Smartphone, and off-the-Shelf Electronics." *PLoS ONE* 11(12):1–15. doi: 10.1371/journal.pone.0167583.

Vollmer, Michael, and Klaus Peter Möllmann. 2018a. "Slow Speed - Fast Motion: Time-Lapse Recordings in Physics Education." *Physics Education* 53(3):1–11. doi: 10.1088/1361-6552/aaa954.

Vollmer, Michael, and Klaus Peter Möllmann. 2018b. "Time-Lapse Videos for Physics Education: Specific Examples." *Physics Education* 53(3):1–11. doi: 10.1088/1361-6552/aab6cf.

Yang, Jun, Man Woo Park, Patricio A. Vela, and Mani Golparvar-Fard. 2015. "Construction Performance Monitoring via Still Images, Time-Lapse Photos, and Video Streams: Now, Tomorrow, and the Future." *Advanced Engineering Informatics* 29(2):211–24. doi: 10.1016/j.aei.2015.01.011.